Aeronautical Research Institute, University of Tokyo
Report No. 364, April 1961

Experimental Investigation of Flow Separation Associated with a Step or a Groove

By

Itiro TANI, Matsusaburo IUCHI
and Hiroyuki KOMODA*

Summary. Low-speed measurements were made on the flow separation associated with a backward-facing step or a rectangular groove by determining the distribution of pressure along the surface and the distributions of mean and fluctuating velocities across several transverse sections. The pressure distribution was found to be rather insensitive to the changes in step height and thickness of the approaching boundary layer. This can be understood by realizing that the cavity flow behind the step is maintained in equilibrium such that the pressure exerted by the solid surface is balanced by the turbulent shear stress, which is set up in the mixing region approximately independently of the step height and the approaching boundary layer. The flow over a groove is markedly different according as it is deep or shallow, the demarcating value of depth-breadth ratio being around 0.7. The deep-groove type of flow is characterized by a comparatively smooth flow and a low value of pressure drag. The converse is true of the shallow grooves. The cavity flow region inside the groove is maintained in equilibrium similarly as in the case of flow over a step.

INTRODUCTION

In view of the importance of the base pressure problem at supersonic speeds, considerable attention has been drawn to the mechanism of flow separation over a sharp edge, the separation being characterized by the formation of reverse flows and vortices, namely *cavity flows*. In particular, Crocco and Lees [*2*] applied to the base pressure problem their general theory based on a flow model exhibiting interaction between the dissipative cavity flow region and the nearly isentropic main flow. Their results could give the qualitative explanation for the observed phenomena. More recently, Korst [*6*] and Chapman, Kuehn and Larson [*7*] independently put forward a simple method of predicting the base pressure by dividing the flow into the cavity flow region in which the pressure is assumed to be constant and the reattachment zone in which the compression is assumed to be such that not much total pressure is lost along the dividing streamline (Figure 1).

It appears from these theoretical investigations that the most essential and intriguing part of the problem is concerned with the mixing process between the dissipative cavity flow and the non-dissipative main flow. But there exists at

* Department of Mechanical Engineering, Nihon University

present little quantitative information about the mechanism of the mixing process. The models used in supersonic measurements have been too small to permit a detailed investigation of the flow inside the mixing region.

This kind of interactive mixing is not confined to supersonic flows; it occurs equally at subsonic speeds. Nevertheless, no *ad hoc* measurement seems to have been made even at subsonic speeds. Some results are given for the subsonic flow over a step, groove, or other surface irregularities in two papers by Wieghardt [*3*] and Tillmann [*4*], where the principal interest centers around the drag increase caused by the irregularities. The flow over a rectangular groove is described by Roshko [*5*] by his results of pressure and mean-velocity measurements. The drag increase is almost entirely accounted for by the pressures on the groove walls. To all seeming the pressure forces being too large to be balanced by the shear forces, Roshko has cast a doubt as to whether the fluid in the cavity flow might be considered to be isolated from the main flow. However, no measurement was made on the shear stress in the mixing region.

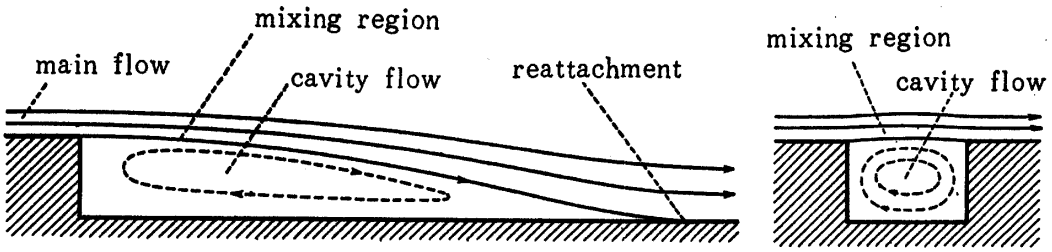

FIGURE 1. Sketches illustrating the flow over a backward-facing step and the flow over a rectangular groove.

In view of these circumstances, the investigation described in this paper was undertaken by determining at subsonic speeds the distribution of surface pressure and that of mean and fluctuating velocities in the flow over a backward-facing step and the flow over a rectangular groove. The work was conducted with the financial support of the Ministry of Education by the Scientific Research Fund. The authors wish to express their indebtedness to Mr. Y. Matsubara, Mr. I. Shimizu and Mr. Y. Komatsu for their cooperation in carrying out the experiments.

A shortened account of the investigation on the flow over a step was presented by Tani at the Symposium on Boundary Layer Research held at Freiburg i. Br., Germany, in August of 1957 [*8*].

EXPERIMENTAL PROCEDURES

The measurements were made in a closed channel of 1- by 1-meter cross section placed within a 1.5-meter low-speed wind tunnel, in which the flat-plate transition Reynolds number was 1.7×10^6. A two-dimensional plate 10 centimeters thick and 190 centimeters long was spanned across the test section. A backward-facing step of adjustable height h (up to 6 centimeters) was made on one side of the plate at a distance of 80 centimeters from the leading edge (Figure 2).

Most of the measurements were made at a main-flow reference velocity U_0 of 28 meters per second, which was actually determined by the static pressure hole located 3 centimeters upstream of the step shoulder, the total pressure being measured outside the boundary layer. Some additional measurements were made, for comparison, at $U_0=22$, 16 and 10 meters per second. The boundary layer 3 centimeters upstream of the step was found to be laminar only at the lowest velocity ($U_0=10$ meters per second), having a thickness of 0.6 centimeter. At the higher velocities the boundary layer was turbulent, and the thickness was 1.1 centimeters for $U_0=28$ meters per second. The boundary layer thickness could be increased to 3 centimeters at $U_0=28$ meters per second by placing a trip 0.5 centimeter high at the distance of 6 centimeters from the leading edge.

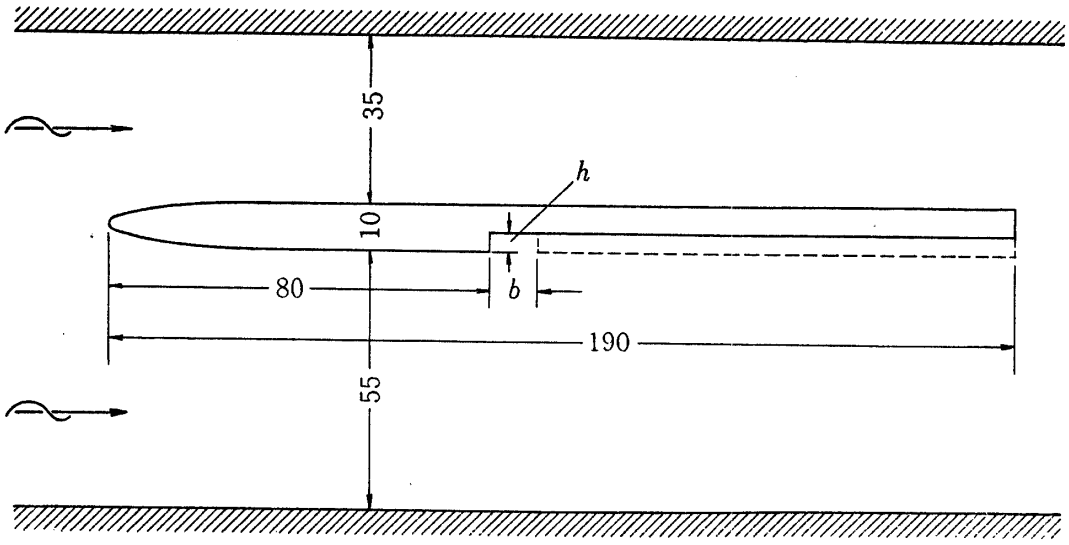

FIGURE 2. Side view of arrangement of the plate with a backward-facing step in the wind channel. Dotted lines are for the arrangement of a rectangular groove. Dimensions in centimeters.

The static pressure was measured by the pressure holes on the model surface and by a small static pressure probe within the mixing region. It was required to aline the probe approximately with the flow direction in order to minimize the error. The total pressure and flow direction were measured by the combined use of two small pitot probes, the one with normal end and the other with slanted end cut 45 degrees from the probe axis. The use of static pressure probe and the slanted pitot probe being questioned in the highly turbulent region, the hot-wire apparatus was also employed for determining mean and fluctuating velocities. The magnitude of mean velocity and the longitudinal component of fluctuating velocity were measured by the usual application of a hot-wire. The transverse components of mean and fluctuating velocities were obtained by setting a hot-wire inclined at two different angles with the flow direction. From these data, determination was made of the distribution of static pressure along the surface, and the distributions of longitudinal mean velocity, mean flow direction, turbulence intensity and turbulent shear stress across the mixing region. It was found that the slanted pitot probe indicated the mean flow direction agreeing well with that

determined by the hot-wire in the outer part of the mixing region, where the turbulence intensity was small, while the indication was somewhat excessive in the highly turbulent central region. Therefore, only the hot-wire results were adopted for the mean flow direction. It is moreover to be noted that the measurements could not be extended into the interior of the cavity flow, where the mean velocities were small, while the fluctuating velocities were comparatively large.

For visualizing the flow pattern, additional observations were made by towing another model in a water tank 1.5 meters wide. The towing velocity was about 15 centimeters per second. The streamlines were made visible by strewing aluminum powders over the water surface, and pictures were taken by a camera moving with the model.

A rectangular groove was made on the same plate in the wind tunnel as shown in Figure 2. The depth h had a fixed value of 4 centimeters, while the breadth b was varied from 2 to 10 centimeters to obtain the depth-breadth ratio h/b ranging from 2 to 0.4. Measurements were made at a main-flow reference velocity U_0 of 28 meters per second, which is the velocity outside the boundary layer at the station located 3 centimeters ahead of the upstream edge of the groove. The boundary layer approaching the groove was turbulent, having a thickness of 1.1 centimeters at the reference station. Pressure holes were made on the model surface to obtain the distribution of static pressure, while the hot-wire apparatus was employed to determine the distributions of longitudinal mean velocity, mean flow direction, turbulence intensity and turbulent shear stress across the mixing region.

Flow over a Step

Experimental results

Figures 3 to 6 show the pressure distribution on the step face as well as on the bottom surface, plotted on the same abscissa. In these results, the distance x measured along the surface is expressed in terms of the step height h, and the pressure p in the form of the pressure coefficient, $C_p=(p-p_0)/\frac{1}{2}\rho U_0^2$, where ρ is the air density, and p_0 and U_0 are the static pressure and main-flow velocity, respectively, at the location 3 centimeters ahead of the step. The values of x/h lying between -1 and 0 correspond to the locations on the step face, while the positive values of x/h to those on the bottom surface.

A remark has to be made with reference to the stability of flow. In each single run of measurement, the pressure observed on the manometer was comparatively steady. But the repeated measurement sometimes yielded a slightly different pressure distribution, indicating the possibility of more than one types of flow pattern under the same boundary conditions. This appears to be typical of the flow separation associated with a step. As a matter of fact, however, the difference in pressure distribution was rather small. The results presented here are those obtained by averaging the data of at least five runs of measurements.

Figures 3 and 4 show the pressure distribution for several different step heights

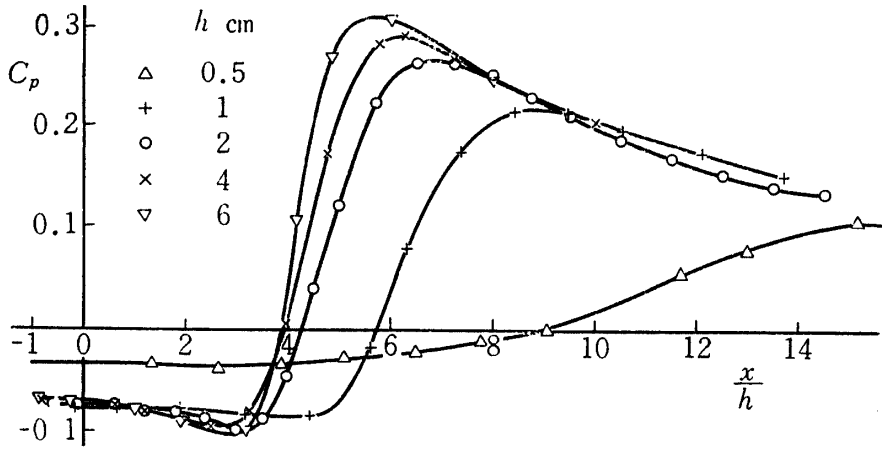

FIGURE 3. Pressure distribution on the step face and the bottom surface for various step heights. $U_0=10$ meters per second.

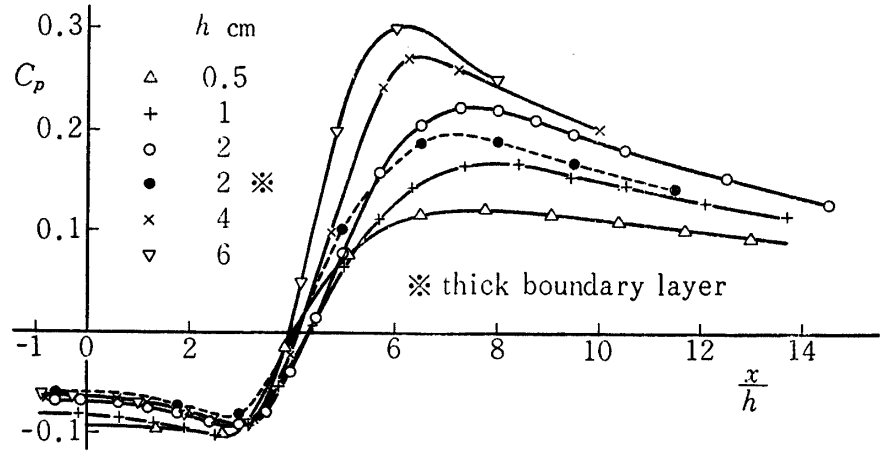

FIGURE 4. Pressure distribution on the step face and the bottom surface for various step heights. $U_0=28$ meters per second.

for $U_0=10$ and 28 meters per second, respectively. As mentioned above, the boundary layer approaching the step is laminar at $U_0=10$ meters per second and turbulent at $U_0=28$ meters per second. The results of similar measurements for $U_0=16$ and 22 meters per second are not shown, because they almost agree with those for $U_0=28$ meters per second. Figure 4 also includes measurements for the case of artificially thickened boundary layer (thickness 3 centimeters). In all cases, there is a negative pressure on the step face (negative base pressure), followed initially by a slight drop in pressure downstream of the step, and then by a rather rapid rise of pressure indicating the reattachment of separated flow.

It is seen from these results that the pressure distribution is rather insensitive to the changes in the step height as well as in the thickness of the approaching boundary layer. In particular, the base pressure is essentially the same for different step heights except for very low steps, and the pressure rise by reattachment increases slightly as the height increases.

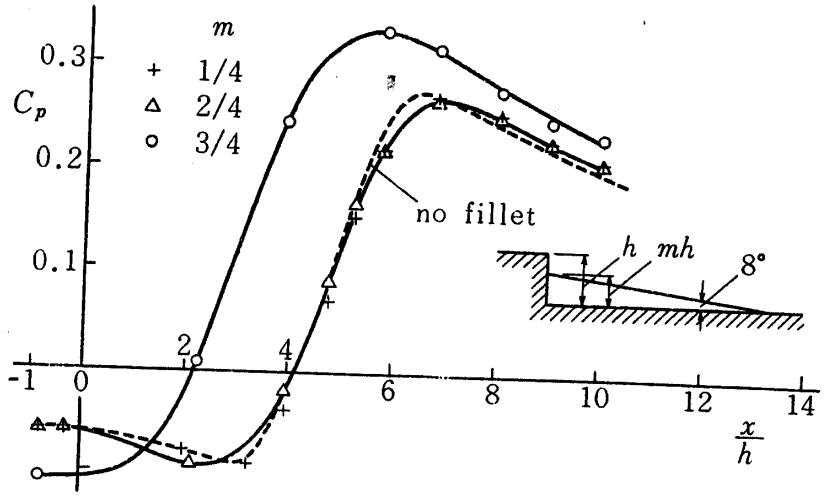

FIGURE 5. Pressure distribution on the step with a triangular fillet. h=4 centimeters, U_0=28 meters per second.

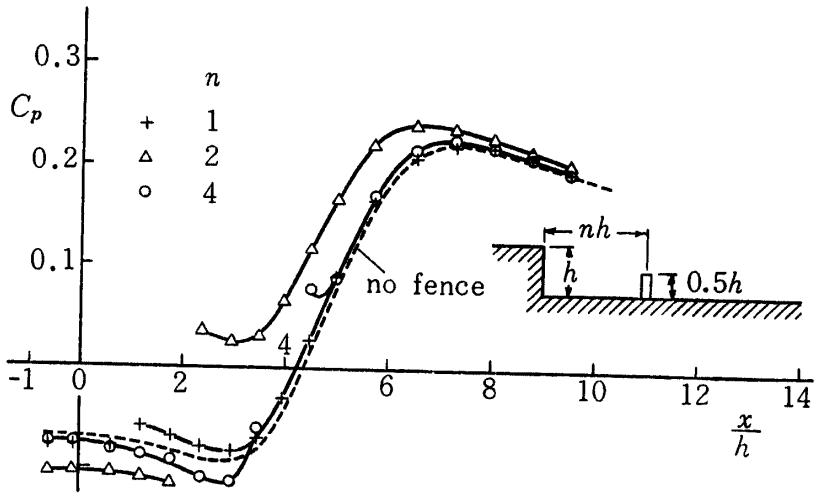

FIGURE 6. Pressure distribution on the step with a fence on the bottom surface. h=2 centimeters, U_0=28 meters per second.

Figure 5 shows the pressure distribution for the cases when a triangular fillet of various heights is inserted behind the step. No appreciable change is observed in the pressure distribution until the fillet height exceeds one half of the step height. Figure 6 shows the pressure distribution for the cases when a fence of the height of one half the step height is placed at various positions on the bottom surface. The effect of the fence is most appreciable when it is placed at a distance of twice the step height from the step.

Figures 7 and 8 show the distribution of longitudinal component of mean velocity U across several transverse sections in the mixing region for U_0=28 meters per second and h=2 and 4 centimeters, respectively. The result also includes the

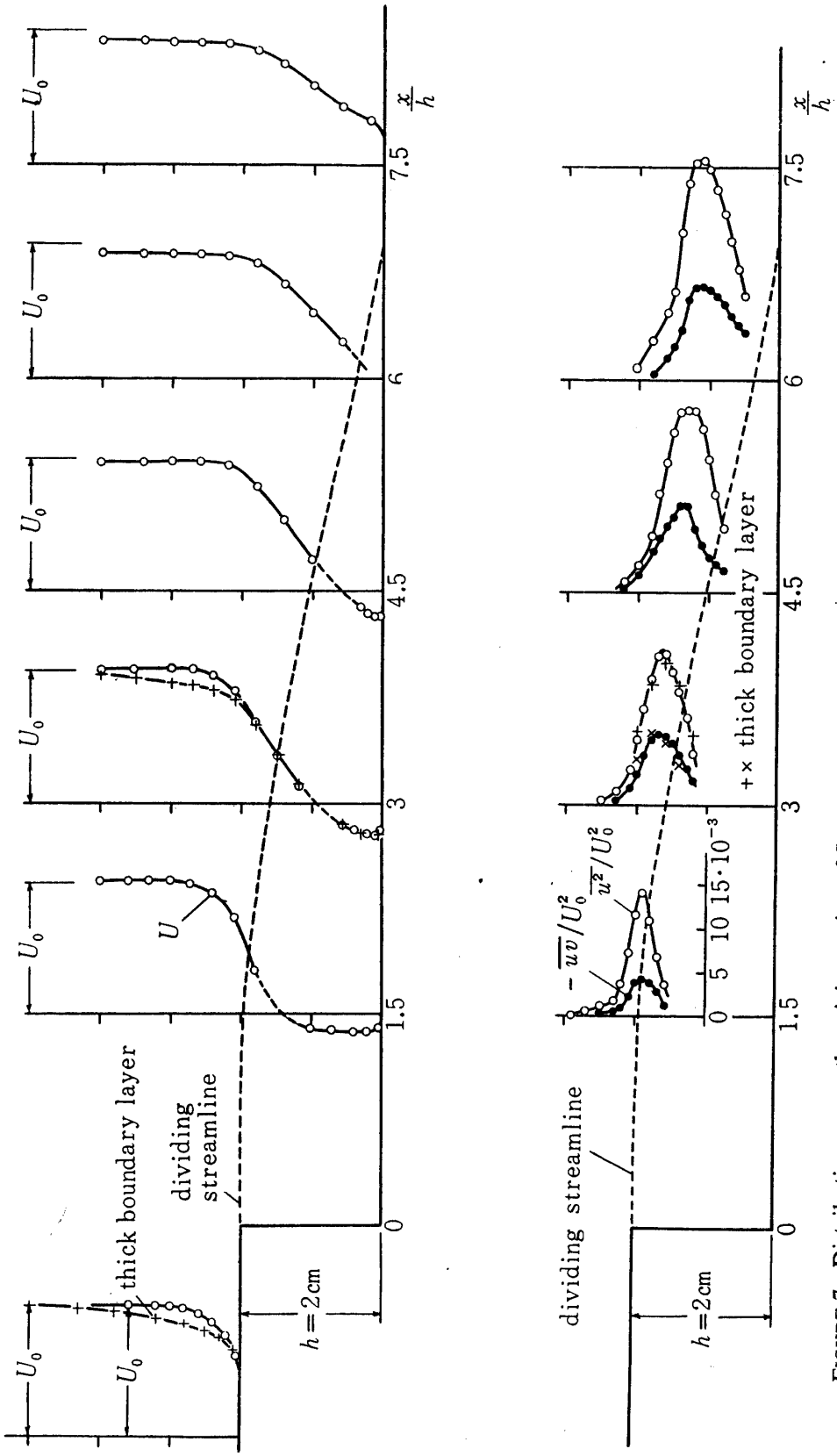

FIGURE 7. Distribution across the mixing region of flow over a step of longitudinal component of mean velocity (upper part), turbulence intensity and turbulent shear stress (lower part). $h=2$ centimeters, $U_0=28$ meters per second.

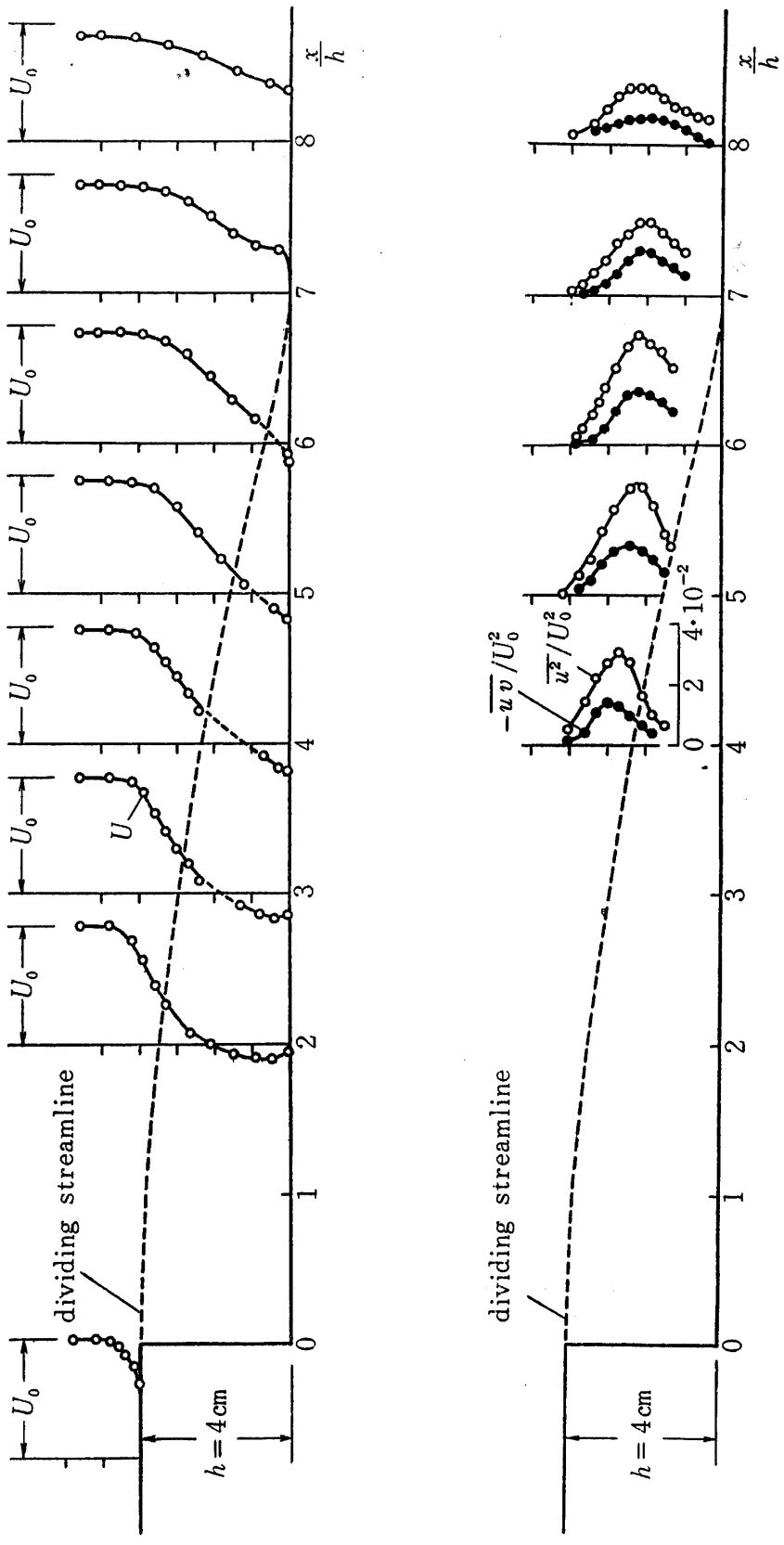

FIGURE 8. Distribution across the mixing region of flow over a step of longitudinal component of mean velocity (upper part), turbulence intensity and turbulent shear stress (lower part). $h=4$ centimeters, $U_0=28$ meters per second.

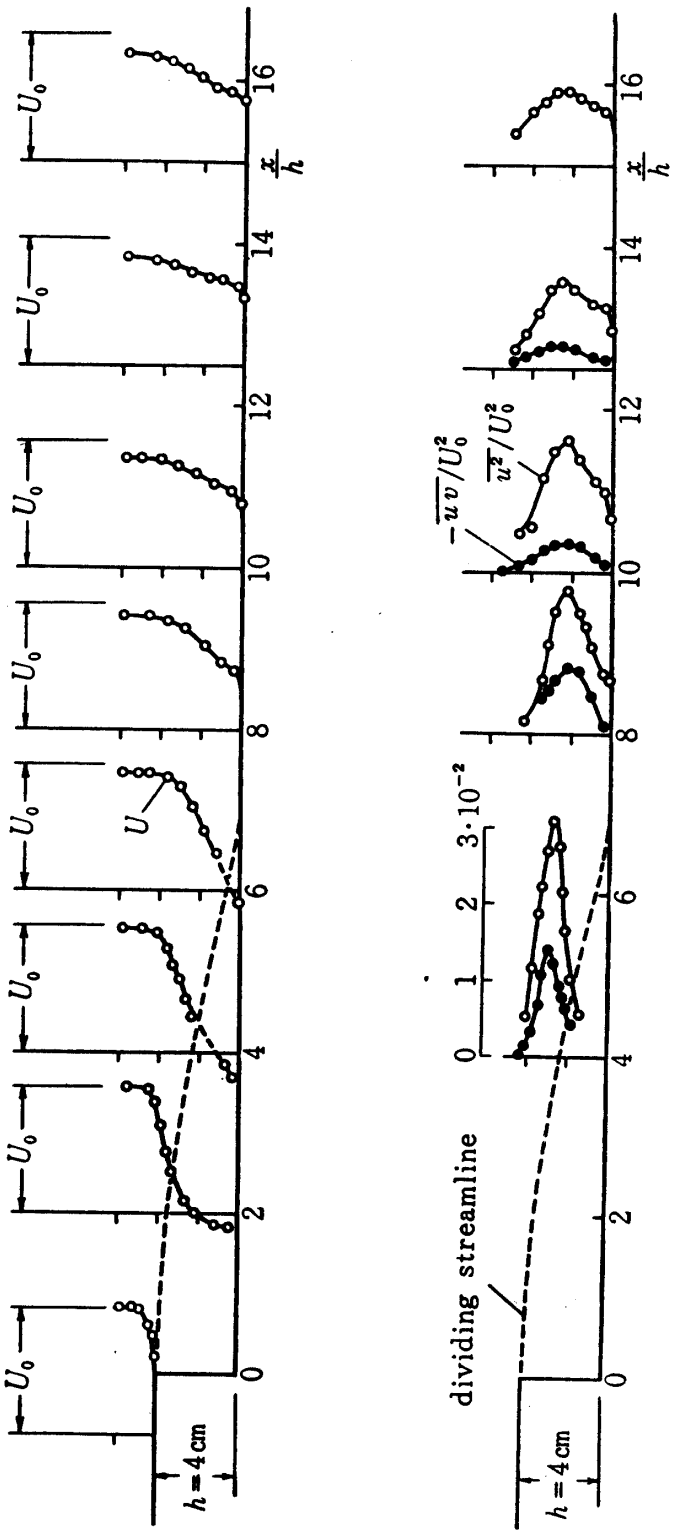

FIGURE 9. Distribution across the mixing region and reattached layer of flow over a step of longitudinal component of mean velocity (upper part), turbulence intensity and turbulent shear stress (lower part). $h=4$ centimeters, $U_0=28$ meters per second.

FIGURE 10. Aluminum-powder pictures of streamlines over a step. Exposure time 0.5 (upper) and 5 seconds (lower).

distribution of longitudinal mean velocity in the reverse flow region immediately close to the bottom surface. Only a rough estimate can be made for the velocity distribution across the central part of cavity flow by joining the two regions of measurement by dotted lines. From the distribution of mean longitudinal velocity, and also by taking into account of the mean flow direction determined by hot-wire measurements, a mean streamline can be drawn that starts from the step shoulder and approaches the bottom surface in the reattachment region. This line can be considered as that dividing the cavity flow region from the main flow.

Figures 7 and 8 also include the distribution of turbulence intensity $\overline{u^2}$ and turbulent shear stress $-\rho\overline{uv}$ made non-dimensional by U_0^2 and ρU_0^2, respectively, where u and v are the components of fluctuating velocity in the directions parallel and normal to the mean streamline, respectively. It is seen that both the turbulence and shear stress increase downstream in the mixing region and that the positions of maximum turbulence and maximum shear stress approximately coincide at the outset with the mean dividing streamline, but deviate outward as the reattachment is approached.

Another point to be noticed from Figures 7 and 8 is that the distributions across the mixing region of mean velocity, turbulence intensity and shear stress are quite insensitive to the changes in the step height as well as in the thickness of the approaching boundary layer.

Figure 9 shows the result of similar measurements extended to the more downstream stations for $h=4$ centimeters. The turbulence and shear stress set up by the flow in the mixing region decrease downstream in the boundary layer initiated by the reattachment of separated flow. On the other hand, a new system of turbulence and shear stress grows up in the reattached layer, until a fully developed turbulent boundary layer having a maximum shear stress at the surface is established at some distance from the reattachment location.

Figure 10 shows the aluminum-powder pictures of streamlines for the step of 5-centimeter height, the exposure time being 0.5 and 5.0 seconds, respectively. The picture of short exposure reveals the intermingling of distinct eddies in cavity flow region, while that of long exposure indicates something like the mean dividing streamline. The Reynolds number based on h and U_0 concerning the water-tank experiments are one order of magnitude lower than those of the wind-tunnel experiments. In view of the above mentioned small effect of Reynolds numbers, however, the flow patterns indicated by aluminum powders are expected to be not much different from those of the wind-tunnel experiments.

Discussions

As mentioned above, the base pressure is essentially the same for different values of step height and boundary layer thickness. Even the difference in character of the approaching boundary layer flow, laminar or turbulent, makes no essential difference except for the step of very small height. This is conceivable because the laminar boundary layer when separated becomes turbulent over a very short distance. For $h=2$ centimeters and $U_0=10$ meters per second, for

example, the transition to turbulence was observed to take place in the separated layer over a distance of only 2 centimeters from the step shoulder.

The base pressure, and also the pressure rise by reattachment, are hardly affected even by the insertion of a triangular fillet behind the step. This suggests that the interaction between the cavity flow and the external flow remains unchanged unless the cavity flow region is unduly oppressed. On the other hand, a considerable change in pressure distribution is found when the reverse part of the cavity flow is interrupted by means of a fence. It is to be noted that the maximum velocity of the uninterrupted reverse flow is about one fourth of the main-flow velocity.

The above mentioned approximate similarity and the comparatively steady character of cavity flow seems to be typical of the flow separation associated with a step. This has tempted one to calculate the flow pattern as the irrotational motion of an inviscid fluid, the cavity flow being replaced by a point vortex captured behind the step. The calculation has been carried out by transforming the physical z-plane conformally into the auxiliary t-plane (Figure 11), and

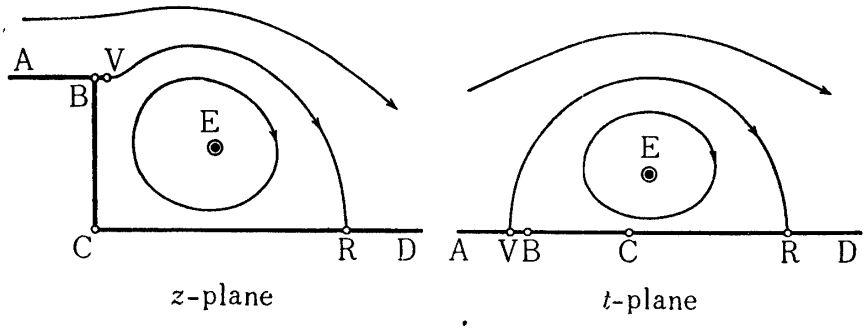

FIGURE 11. Flow pattern around a step based on the irrotational motion of an inviscid fluid in the physical z-plane and the auxiliary t-plane.

requiring that the vortex is at rest and that the velocity at the visor tip V has a nonzero finite value equal to the undisturbed velocity.* It is found that the vortex is stable against small disturbances and that the required length of visor, BV, is only one twentieth of the step height, BC. Yet the result of calculation is at variance with the measurement; the streamline leaving the visor tip rises upward considerably so that the distance to reattachment, CR, is predicted to be only 1.67 times the step height, while the observed value is about 7 times the step height.

A correct understanding may probably be obtained by realizing that the cavity flow is chiefly maintained by the turbulent shear stress, which is set up in the mixing region approximately independently of the characteristics of the approaching boundary layer. This view seems to be supported by the observed result that the distribution of $-\overline{uv}/U_0^2$ is hardly affected by the artificial thickening of the approaching boundary layer (Figure 7). It is moreover to be remembered that the

* If there were no visor, the step shoulder B would become a stagnation point.

distribution of $-\overline{uv}/U_0^2$ for the step of 2-centimeter height is not appreciably different from that for the step of 4-centimeter height (Figures 7 and 8).

The model of the flow pattern might be simplified if the cavity flow were considered to be isolated from the main flow by the above mentioned mean dividing streamline. Aluminum-powder picture such as the lower part of Figure 10 appears more likely to favor the possibility of isolation. If this were the case, the normal and tangential stresses acting on the boundary of the cavity flow region should be in equilibrium, because otherwise a certain amount of momentum should be transported into or out of the region.

From the results of measurements for $h=2$ centimeters and $U_0=28$ meters per second, a rough examination can be made for the equilibrium of the stresses acting on the fluid in cavity flow. The pressure force exerted by the step face is -0.07, when made non-dimensional by the step height h and the dynamic pressure $\frac{1}{2}\rho U_0^2$. Negative sign indicates that the force is against the direction of undisturbed main flow. Similarly, the pressure force acting on the dividing streamline is -0.03. The shear force exerted by the bottom surface is $+0.01$, which is estimated from the velocity distribution of the reverse flow. Finally, the shear force acting on the dividing streamline is $+0.07$. The sum of these force is not exactly equal to zero, but sufficiently small so that the forces can be considered to form approximately a system of equilibrium.

According to the experiments of Liepmann and Laufer [*1*], the turbulent shear stress in a half jet increases at the outset, but tends to maintain a constant value after a certain distance is covered. As indicated above, however, this is not the case for the separated flow over a step, the shear stress continuing to increase in the mixing region so as to make an equilibrium possible of the stresses acting on the fluid in cavity flow. Undoubtedly the development of shear stress is considered to be consequent upon the interaction between the dissipative cavity flow and the non-dissipative main flow.

Flow over a Groove

Experimental results

Figure 12 shows the pressure distribution on the groove walls as well as on the bottom surface, plotted on the same abscissa, for the grooves of depth-breadth ratios $h/b=2.0$, 1.0, 0.8, 0.5 and 0.4. In these results, the pressure p is made non-dimensional in the form of the pressure coefficient, $C_p=(p-p_0)/\frac{1}{2}\rho U_0^2$, where p_0 and U_0 are the static pressure and main-flow velocity, respectively, at the location 3 centimeters ahead of the upstream shoulder of the groove.

The pressure distributions are of rather mazy shape, indicating the complicated structure of cavity flow inside the groove. The pressure is mostly negative on the upstream wall and the bottom surface, while it is mostly positive or negative on the downstream wall according as the groove is shallow or deep. In all cases there is a steep rise in pressure near the downstream shoulder, consequent upon the stagnation of the flow separated at the upstream shoulder. The maximum

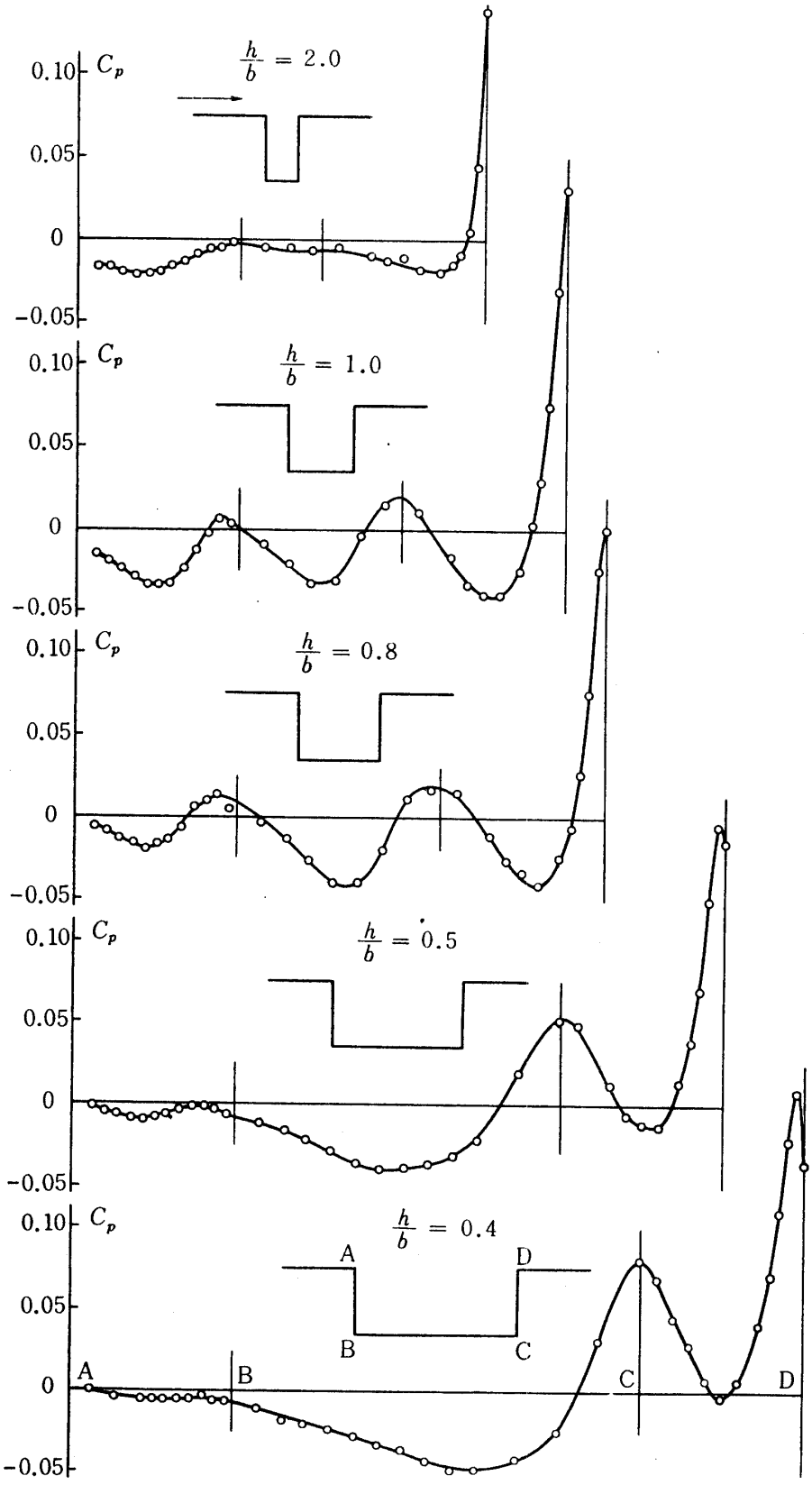

FIGURE 12. Pressure distribution on groove walls and bottom surface for grooves of various depth-breadth ratios. h=4 centimeters, U_0=28 meters per second.

pressure is located at the downstream shoulder for deep grooves, but displaced slightly downward as the depth-breadth ratio is reduced.

Figure 13 show the integrated mean values of C_p over the upstream and downstream walls, $\hat{C}_{p(u)}$ and $\hat{C}_{p(d)}$, respectively, plotted against the depth-breadth ratio h/b. The shear stress acting on the bottom surface being negligibly small, the difference $\hat{C}_{p(d)}-\hat{C}_{p(u)}$ accounts for most of the drag experienced by the groove, made non-dimensional by the depth h and the dynamic pressure $\frac{1}{2}\rho U_0^2$. This non-dimensional drag coefficient, denoted by C_D, is also shown in Figure 13.

These results of pressure measurements are in fair agreement with those previously obtained by Roshko [5]. The comparison is made for the drag coefficient C_D in Figure 13.

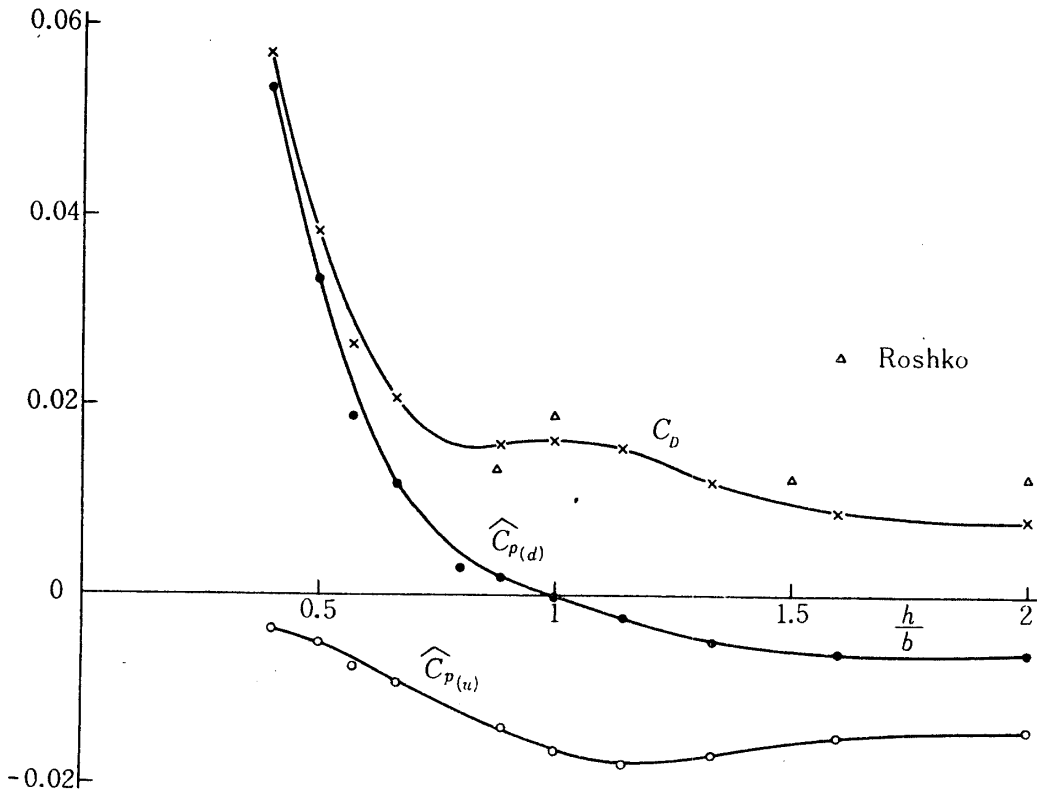

FIGURE 13. Pressure forces on groove walls for grooves of various depth-breadth ratio. h=4 centimeters, U_0=28 meters per second.

Figure 14 shows the distributions across several transverse sections for the square groove ($h/b=1$) of longitudinal component of mean velocity U, turbulence intensity $\overline{u^2}$ and turbulent shear stress $-\rho\overline{uv}$, made non-dimensional by U_0, U_0^2 and ρU_0^2, respectively, where u and v are the longitudinal and transverse components of fluctuating velocity, respectively. Figure 15 shows the results of similar measurements for the groove of $h/b=0.4$. The important point to note in these figures is that the turbulence and shear stress set up in the mixing region in the shallow groove ($h/b=0.4$) are stronger than those in the square groove.

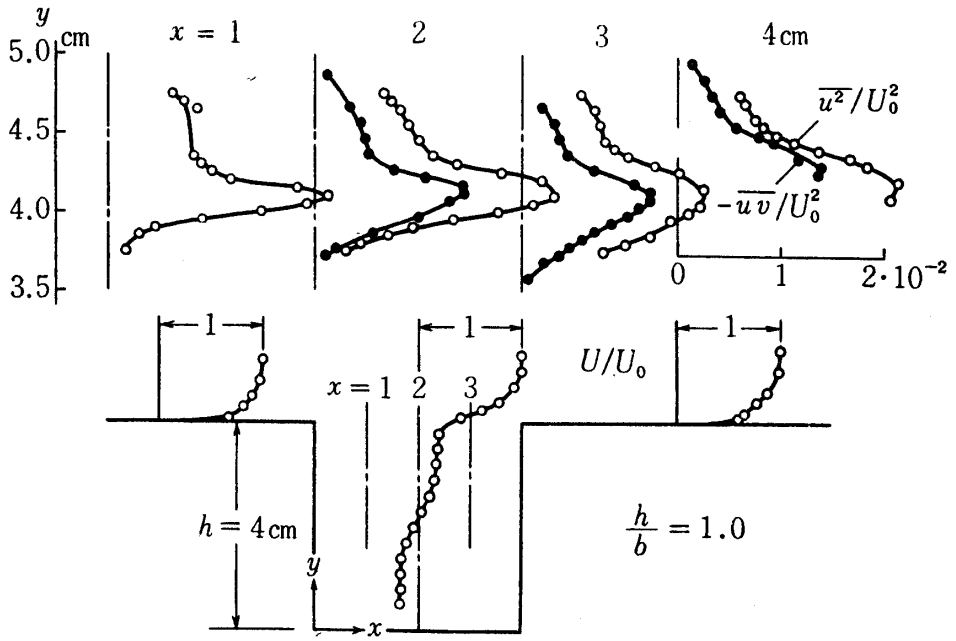

FIGURE 14. Distribution across several transverse sections of flow over a groove of longitudinal component of mean velocity, turbulence intensity and turbulent shear stress. $h/b=1.0$, $U_0=28$ meters per second.

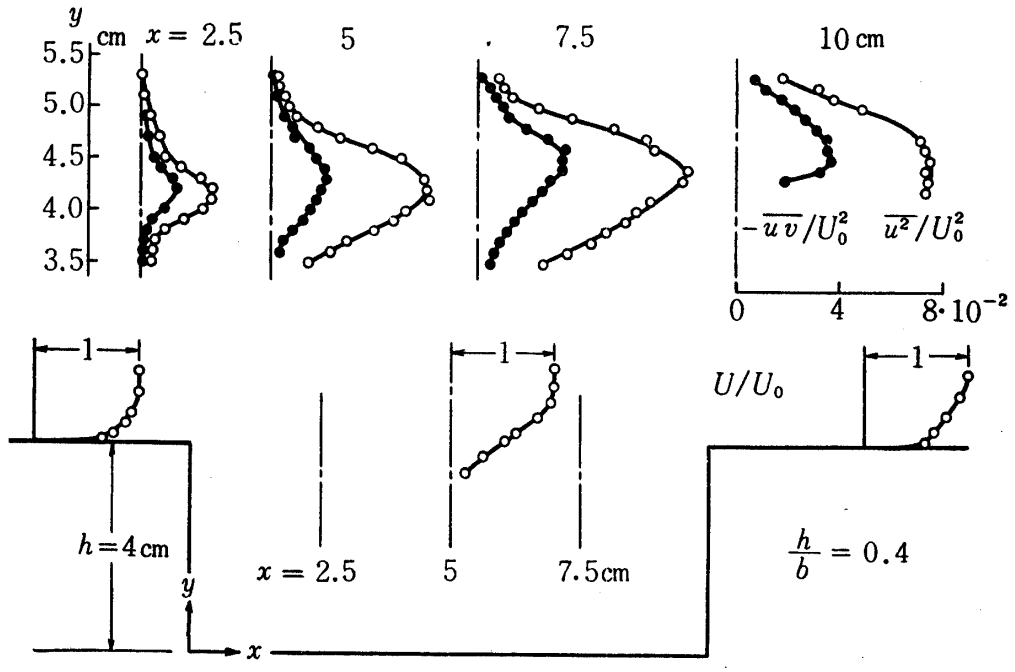

FIGURE 15. Distribution across several transverse sections of flow over a groove of longitudinal component of mean velocity, turbulence intensity and turbulent shear stress. $h/b=0.4$, $U_0=28$ meters per second.

In common with the flow over a step, there exists the possibility of more than one types of flow pattern for a given groove. Each type of flow pattern yields a definite pressure distribution slightly different each other. The difference being comparatively small, the results are presented that are obtained by averaging the data of at least five runs of measurements.

Discussions

In the range of depth-breadth ratio h/b covered by the present investigation, it appears that the groove may be broadly divided into *deep* and *shallow*, the demarcating value of h/b lying around 0.7. In *deep* grooves, the maximum pressure on the downstream wall is found at the shoulder, indicating a smooth flow passing over the shoulder. The groove drag coefficient C_D is small and decreases as h/b increases. In *shallow* grooves, the maximum pressure occurs slightly below the shoulder of the downstream wall. This is indicative of a less smooth flow around the shoulder and corroborated by the higher values of the drag coefficient C_D.

As mentioned above with the flow over a step, there is good reason for assuming that the stresses acting on the fluid in cavity flow are in equilibrium. Then the pressure force exerted by the groove walls, which is given by $-C_D$, is to be balanced by the shear force acting on the free side of cavity flow, namely the mean dividing streamline. In the measurement of the shear stress distribution along the normal to the groove bottom, however, there was a difficulty in locating the transverse coordinate with sufficient accuracy. Moreover, the mean dividing streamline could be drawn only in a loose sense, because of the difficulty of determining the mean velocity distribution in the cavity flow region. For these reasons, it is not easy to make a reliable estimate for the shear force acting on the dividing streamline. Nevertheless, a brief examination of Figures 14 and 15 is sufficient to estimate the shear force to be of the proper order of magnitude to balance the pressure force exerted by the walls.

The flow over a shallow groove is less smooth as compared with that of a deep groove. This is corroborated by the increase in fluctuation of pressure observed on the manometer. One is then liable to surmise that the fluid in a shallow groove is not in equilibrium. But that is not a supposable case. When averaged over a sufficient length of time, the transport of momentum into the groove is to be balanced by the force exerted by the groove walls. The time average of momentum transport presents itself in the form of high shear stress in the mixing region. It is the authors' viewpoint that the turbulent shear stress is necessarily set up in the mixing region in such a way that the forces acting on the fluid form a system of equilibrium.

Conclusion

The low-speed measurements on the flow separation associated with a backward-facing step or a rectangular groove bring out the following features:

1. Except for steps of very small height, the base pressure is essentially the

same for different values of step height and boundary layer thickness, and the pressure rise by flow reattachment increases slightly as the step height is increased or the boundary layer thickness is reduced.

2. The base pressure and the pressure rise by reattachment are almost unchanged even when a triangular fillet is inserted behind the step. An appreciable change in pressure distribution is found, however, when the reverse part of cavity flow is interrupted by placing a fence on the bottom surface.

3. The insensitivity of base pressure to the step height and boundary layer thickness can be explained by realizing that the cavity flow is chiefly maintained by the turbulent shear stress, which is set up in the mixing region approximately independently of the step height and the approaching boundary layer. The shear stress amounts to a value large enough to balance the pressure force exerted by the solid surface.

4. From the viewpoint of flow patterns, the rectangular groove may be broadly divided into deep and shallow, the demarcating value of depth-breadth ratio being around 0.7. In deep grooves, the separated flow passes over smoothly and the pressure drag experienced by the groove is small. The converse is true of the shallow grooves. In any case, the shear stress developed in the mixing region amounts to a value large enough to balance the pressure drag.

Department of Aerodynamics
Aeronautical Research Institute
University of Tokyo, Tokyo
February 22, 1961

References

[1] Liepmann, H. W., and Laufer, J.: Investigations of Free Turbulent Mixing. N. A. C. A. Tech. Note No. 1257, 1947.

[2] Crocco, L., and Lees, L.: A Mixing Theory for the Interaction between Dissipative Flows and Nearly Isentropic Streams. J. Aero. Sci., Vol. 19, pp. 649–676, 1952.

[3] Wieghardt, K.: Erhöhung des turbulenten Reibungswiderstandes durch Oberflächenstörungen. Forschungshefte für Schiffstechnik, Heft 2, pp. 65–81, 1953.

[4] Tillmann, W.: Neue Widerstandsmessungen an Oberflächenstörungen in der turbulenten Reibungsschicht. Forschungshefte für Schiffstechnik, Heft 2, pp. 81–88, 1953.

[5] Roshko, A.: Some Measurements of Flow in a Rectangular Cutout. N. A. C. A. Tech. Note No. 3488, 1955.

[6] Korst, H. H.: A Theory for Base Pressures in Transonic and Supersonic Flow. J. App. Mech., Vol. 23, pp. 593–600, 1956.

[7] Chapman, D. R., Kuehn, D. M., and Larson, H. K.: Investigation of Separated Flows in Supersonic and Subsonic Streams with Emphasis on the Effect of Transition. N. A. C. A. Tech. Note No. 3869, 1957.

[8] Tani, I.: Experimental Investigation of Flow Separation over a Step. Grenzschichtforschung, Symposium Freiburg i. Br., August 1957, pp. 377–386. Berlin-Göttingen-Heidelberg 1958.

概　要

ステップまたは溝による流れの剝離の実験的研究

谷　一郎・井内松三郎・菰田廣之

後向きステップまたは長方形の溝による流れの剝離について，壁面に沿う圧力分布ならびにいくつかの横断面での平均および変動速度の分布を低速風路で測定した．ステップの圧力分布は，ステップの高さまたはステップ上流の境界層の厚さの変化によって，あまり大きな影響を受けることがない．これはステップの後に生ずるくぼみ流れ（腔流）の平衡が保たれ，それにはたらく壁面の圧力と，ステップの高さおよびステップ上流の境界層にほぼ無関係に混合領域に発生する乱流剪断応力が釣合うことを考えると理解できる．溝を越える流れは，溝が深いか浅いかによって著しく異なるが，その境目は溝の深さと幅の比がおよそ 0.7 の附近にある．深い溝の場合には，流れは比較的に滑かで，圧力抵抗は小さい．浅い溝では反対である．溝の中のくぼみ流れは，ステップの場合と同じようにその平衡が保たれる．